

VICARIOUS CALIBRATION OF GLOBAL PRECIPITATION MEASUREMENT MICROWAVE RADIOMETERS

Darren McKague
Chris Ruf
John J. Puckett
University of Michigan

ABSTRACT

The vicarious cold calibration method of Ruf has been used to assess the calibration of the TMI, WindSat, SSM/I F13 and SSM/I F14 microwave radiometers using data from the GPM Inter-Calibration Working Group. Significant scan position dependent biases are seen for TMI (as large as 1 K) and for WindSat (as large as 5 K) – scan position dependent biases in SSM/I data were removed prior to processing. These biases are thought to be due to obstructions in the edge of scan field of view from the given instrument and its spacecraft. WindSat vertically polarized data also show a linear decrease in vicarious cold calibration brightness temperatures with scan position. SSM/I F13 and F14 vicarious cold brightness temperatures differ by an amount consistent with a $\sim .2^\circ$ offset in their relative Earth incidence angles.

Index Terms— Microwave radiometry, Calibration

1. INTRODUCTION

The primary goal of NASA's Global Precipitation Measurement (GPM) mission is to improve the accuracy, sampling, and coverage of global precipitation measurements. This will be accomplished, in part, with a constellation of space-borne microwave radiometers. Each radiometer will have its own set of radiometric characteristics (viewing geometry, bandwidth, center frequency, for example) and its own error sources. For precipitation estimates from each to be consistent, differences in these radiometric characteristics and error sources must be well known. The goal of the GPM Inter-Calibration Working Group (ICWG) is to understand and quantify, and correct for these differences.

The ICWG is currently focusing on developing the techniques of radiometer inter-calibration through comparison of data from four radiometers currently on-orbit: the Defense Meteorological Satellite Program Special Sensor Microwave/Imager (SSM/I) on the F13 and F14 satellites, the Naval Research Lab WindSat radiometer, and

NASA's Tropical Rainfall Measurement Mission Microwave Imager (TMI). The groups within the ICWG are independently developing methods for producing inter-calibrated measurements for a common data set from these four radiometers. By comparing the data from each radiometer, as well as comparing the different methods of inter-calibration, the working group will develop a method of producing consistent calibrated measurements amongst the radiometers that will comprise the GPM constellation. This paper gives the highlights of the progress to-date of the ICWG group from the University of Michigan (U of M).

2. VICARIOUS COLD CALIBRATION

The U of M approach to radiometer inter-calibration is to adapt the vicarious calibration techniques developed for previous space-borne radiometers (SSM/I, TOPEX, GEOSAT Follow-On, Jason and WindSat) and apply them to the GPM constellation [1, 2]. These techniques provide a means to transfer main beam brightness temperature calibration standards between space-borne radiometers that operate at different frequencies, incidence angles, polarizations and/or orbit geometries. With the vicarious calibration techniques, absolute calibration of the sensors has been demonstrated to 1 K. Relative calibration between sensors, as well as stabilization of a sensor's calibration over time periods of ten years or more, has been demonstrated to 0.3 K [3].

The manner in which the microwave brightness temperature (T_b) of the ocean varies as a function of sea surface temperature (SST), salinity (SSS), near surface wind speed (u) and atmospheric opacity can be taken advantage of as a source of vicarious calibration for an orbiting microwave radiometer. For every microwave frequency, polarization and incidence angle there is a unique combination of SST and SSS at which the T_b of an ideal, flat ocean surface is a minimum. Departures of SST and SSS from that point, as well as all variations in u and atmospheric opacity, will tend to increase the T_b above its theoretical minimum as observed by a downward looking radiometer in Earth orbit.

This work was supported in part by NASA Grant NNX07AD69G.

An inverse cumulative distribution function (ICDF) for T_b can be constructed which has the property that:

$$\text{ICDF}(x) = T_b \text{ for } 0 \leq x \leq 100\%$$

provided $x\%$ of the measurements have values below T_b . The ICDF is the inverse of the standard cumulative distribution function (CDF, the definite integral of the probability density function for T_b). The ICDF can be used to solve for the highest T_b for which $x=0\%$ - the vicarious cold T_b . This vicarious cold T_b has been successfully used as a calibration reference for the TOPEX Microwave Radiometer (TMR) with channels of 18, 21 and 37 GHz at a nadir angle of incidence [3].

3. ICWG VICARIOUS COLD PRELIMINARY RESULTS

The vicarious cold T_b technique has been applied to TMI, WindSat, SSM/I F13, and SSM/I F14 for data from July 1, 2005 to June 30, 2006. These data are screened for land and sea ice using Global Data Assimilation System (GDAS) 6 hourly data, and are screened for precipitation using the rain flags of Stogryn [4]. In Ruf's analysis, a 3rd order polynomial fit to the ICDF between 3% and 10% was used to extrapolate the vicarious cold T_b (at 0%) [1]. For the data here, a 2nd order fit between 2% and 10% was used. These fit parameters were found to provide a set of vicarious cold T_b s with the lowest standard deviation over a subset of data with relatively constant vicarious cold T_b s.

3.1. Scan position biases

With these fit parameters, vicarious cold T_b s were produced as a function of instrument scan position and are shown for each instrument in Figure 1. These cold T_b s are shown as a deviation from the mean cold T_b (cold T_b anomalies). Both SSM/I instruments show little variation with scan position; scan position biases have already been removed from these two based on the analysis of Colton and Poe [5]. No scan position correction has been applied to either WindSat or TMI data.

The most likely cause for the decrease in TMI vicarious cold T_b s near the scan edges is the contamination by emission or scattering into the field of view from the spacecraft and/or instrument structure [5]. Note that the magnitude of the effect increases with decreasing frequency. This makes sense for the proposed cause given the wider beam widths for lower frequency channels – wider beam widths make these channels more susceptible to obstructions near the scan edges which also show up closer to the scan center. Note also that the effect is primarily in the vertically polarized channels. This may be due to the different beam patterns for the vertically (V) and horizontally (H) polarized channels due to their different (orthogonal) orientations relative to the principal planes of the radiometer waveguide.

The vertically polarized beam patterns may have larger side-lobes in the direction of rotation of the radiometer (along-scan) relative to the horizontally polarized channels and are thus more affected by interference in the along-scan direction.

WindSat data show this edge of scan effect for 6 GHz V and H data, and 22 GHz V data. Again, the 6 GHz channel will have the widest beam width so would be most effected by obstructions at the scan edges. This bias is as large as – 5 K (off scale) from the mean for the 6 GHz V channel. Further investigation is needed to explain the edge of scan effect seen in the 22 GHz V data. It may be that there is an obstruction along the scan path of the 22 GHz feed-horn that does not interfere with the other feeds.

Finally, the WindSat vertically polarized channels all show a steady decrease in vicarious cold T_b with increasing scan position. This may be due to Earth incidence angle (EIA) changes across the scan due to an offset in spacecraft attitude. Further investigation is required to pinpoint the source of this bias.

3.3. Sensitivity to EIA

As mentioned above, the SSM/I F13 and F14 data are relatively free of scan position biases. For these, it makes sense to compare the average vicarious cold T_b s at each channel between the two instruments. These T_b s, their standard deviations, and their differences, are given by channel in Table 1. Since the channel center frequencies, band widths, and nominal Earth incidence angles (EIAs) are the same, one would expect, in the absence of any difference in the data themselves, that the vicarious cold T_b s of the two instruments would match to within the noise of the data. As seen in Table 1, they do not.

Table 1. Mean and standard deviation of the vicarious cold T_b s for SSM/I F13 and F14 by channel. The last two rows are the modeled differences with a given difference in EIA between F13 and F14 using the model of Elsaesser [6].

	Vicarious Cold T_b (K)				
	19 V	19 H	22 V	37 V	37H
F13	176.65 ± .07	98.11 ± .14	183.40 ± .12	201.00 ± .05	128.12 ± .12
F14	177.00 ± .05	98.20 ± .15	183.67 ± .12	201.80 ± .03	128.14 ± .09
F14-F13	0.35 ± .12	0.09 ± .29	0.27 ± .24	0.80 ± .08	0.02 ± .21
F14-F13, $\Delta\text{EIA} = .1^\circ$	0.23	-0.12	0.24	0.24	-0.05
F14-F13, $\Delta\text{EIA} = .4^\circ$	0.96	-0.47	0.97	0.95	-0.22

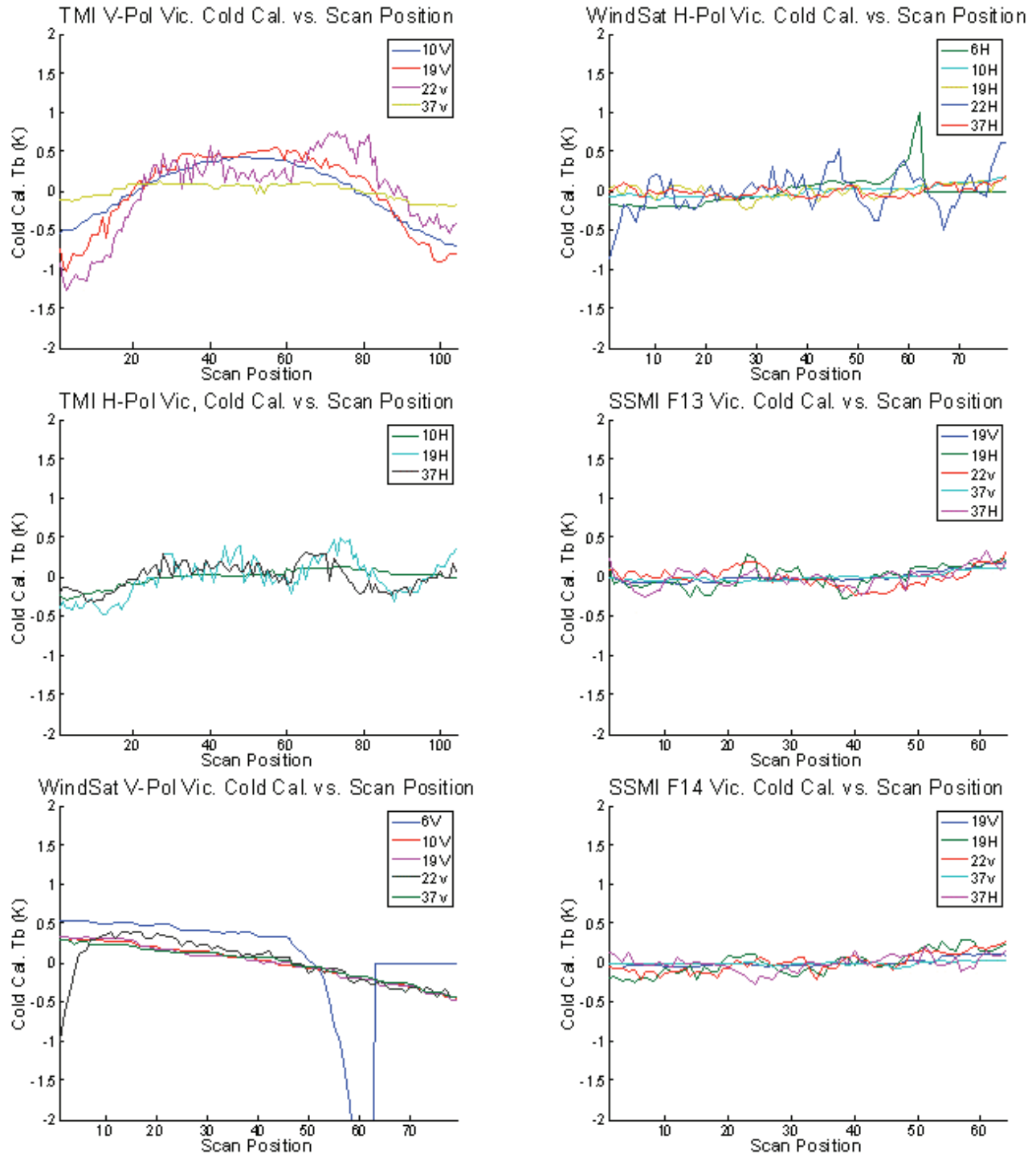


Figure 1. Vicarious cold T_b anomalies (difference from mean) for TMI, WindSat, SSM/I F13 and SSM/I F14 as a function of scan position for data from July 2005 to June 2006. Note that the WindSat 6 GHz scan ends earlier relative to the other channels in these data – at scan position 64 – due to an offset in the alignment of the 6 GHz feed-horn.

5. REFERENCES

Figure 4 shows the relationship between the vicarious cold T_b and EIA by channel for vertically polarized channels. There is a fair bit of sensitivity to EIA at all channels. Horizontally polarized channels look similar but have a negative EIA/vicarious cold T_b slope. Using these relationships, the SSM/I EIAs can be varied from their nominal values to determine if an offset in EIA can explain the differences in vicarious cold T_b s between the F13 and F14 SSM/I. For an EIA offset of between $.1^\circ$ and $.4^\circ$ for F14 relative to F13, the expected difference in vicarious cold T_b s by channel are given in rows 5 and 6 of Table 1. These are in the same range as the observed differences given in row 4. From Colton and Poe [5], the mean EIA of SSM/I F13 and F14 differ by $.3^\circ$.

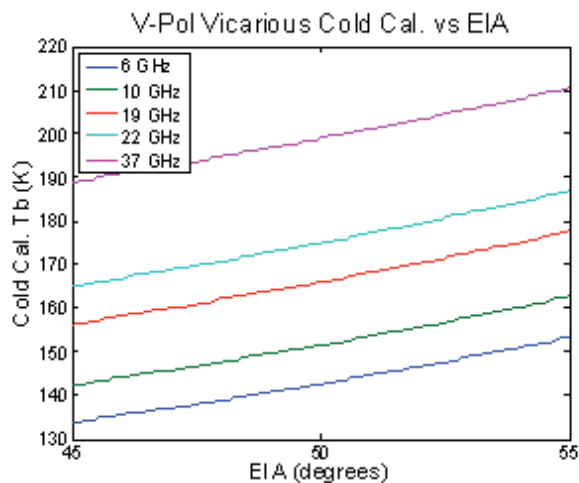


Figure 4. Vicarious cold T_b s as a function of Earth Incidence Angle for vertically polarized channels. Horizontally polarized channels look similar but have a negative EIA/vicarious cold T_b slope. Data are from the model of Elsaesser [6].

4. CONCLUSIONS

The results shown here summarize some of the preliminary analysis by U of M of the calibration of the TMI, WindSat, SSM/I F13 and SSM/I F14 instruments for the GPM ICWG. These analyses based on the vicarious calibration techniques of Ruf show significant scan position biases for TMI (as large as 1 K) and WindSat (as large as 5 K). They also show an EIA offset of around $.3^\circ$ for F14 relative to F13 from the nominal EIA of 53.1° . Future work will look at further instrument to instrument comparisons as well as isolating atmospheric effects and determining the root causes of and eliminating the observed biases.

[1] Ruf, C.S., Y. Hu and S.T. Brown, "Calibration of WindSat Polarimetric Channels with a Vicarious Cold Reference," IEEE Trans. Geosci. Remote Sens., 44(3), 470-475, 2006.

[2] Ruf, C.S. "Detection of calibration drifts in spaceborne microwave radiometers using a vicarious cold reference," IEEE Trans. Geosci. Remote Sens., 38(1), 44-52, 2000.

[3] Ruf, C.S., "Characterization and Correction of a Drift in Calibration of the TOPEX Microwave Radiometer", IEEE Trans. Geosci. Remote Sens., 40(2), 509-511, 2002.

[4] A. P. Stogryn, C. T. Butler, and T. J. Bartolac, "Ocean surface wind retrievals from special sensor microwave/imager data with neural networks," J. Geophys. Res., vol. 90, pp. 981-984, 1994.

[5] Colton, M. C., and G. A. Poe, "Intersensor Calibration of DMSP SSM/I's: F-8 to F-14, 1987 - 1997," IEEE Trans. Geosci. Rem. Sens, 37(1), 418-439, 1999.

[6] Elsaesser, G. S. and C. K. Kummerow, 2007: "Towards a fully parametric retrieval of the non-raining parameters over the global oceans," J. Appl. Meteor. & Climatol., (in press).